Morphology and Corrosion Behavior of Stir-Cast Al6061-CeO_2 Nanocomposite Immersed in NaCl and H_2So_4 Solutions

Kumar, Dinesh
Department of Mechanical Engineering, National Institute of Technology Kurukshetra

Singh, Satnam
Department of Mechanical Engineering, National Institute of Technology Kurukshetra

Angra, Surjit
Department of Mechanical Engineering, National Institute of Technology Kurukshetra

https://doi.org/10.5109/6781054

出版情報：Evergreen. 10 (1), pp.94-104, 2023-03. 九州大学グリーンテクノロジー研究教育センター
バージョン：

Morphology and Corrosion Behavior of Stir-Cast Al6061-CeO_2 Nanocomposite Immersed in NaCl and H_2So_4 Solutions

Dinesh Kumar[1*], Satnam Singh[1], Surjit Angra[1]
[1]Department of Mechanical Engineering, National Institute of Technology Kurukshetra-India

*Author to whom correspondence should be addressed:
E-mail: dinesh_61900120@nitkkr.ac.in

(Received November 25, 2022; Revised February 3, 2023; accepted February 6, 2023).

Abstract: Durability in terms of life is intended as a significant factor in developing advanced materials. The enrichment in corrosion resistance of the produced progressive material can be the solution. In the current study, a nanocomposite of aluminum 6061 and cerium oxide was prepared with a stir casting route reinforced in the range of 1-3 wt.%. The corrosion and microstructural behavior were observed under parametric conditions. The exposure time (36-180 hours), temperatures (room temperature, 45 ºC, and 75 ºC), and 2.5 wt.% of Sodium chloride (NaCl) and Sulphuric acid (H_2So_4) solutions were chosen as parameters for examining the corrosion rate using the immersion test method. The lower corrosion resistance was noticed in aluminum metal matrix nanocomposites (AlMMNCs) reinforced with 3 wt.% of CeO_2. The SEM analysis concluded voids, holes, clustering of particles, and debris kind of defects were observed in stir casting of AlMMNCs samples. The Pitting, fretting, and grain boundary corrosions were the primary degradation factors for corrosion behavior as evaluated from microstructural characteristics. The 0.116 has been observed as a significant corrosion rate in mm potential per year after 180 hours as exposure time at 75ºC in 2.5 wt.% NaCl solution.

Keywords**:** Al-6061, cerium oxide, stir casting, immersion test, morphology, corrosion.

1. Introduction

The use of aluminum and alloys has been considered the primary material for military and civilian aircraft construction of body structures since the Second World War. Other uses for aluminum-based materials are found in the automotive, aerospace, and transportation sectors [1)]. The lower density, combined with the higher strength and stiffness, is a major reason for choosing aluminum as the working material over monolithic materials. Nowadays, this aluminum and alloys are being replaced by metal matrix composites (MMCs). In an MMC, a brace or two is added to an aluminum matrix, creating a new material that has greater strength, stiffness, lower density, and higher corrosion resistance[2)]. The composite with one nano-reinforcement is called aluminum metal matrix nano-composites (AlMMNCs), while the composite with two or more reinforcements added to the aluminum as the matrix material is called hybrid aluminum metal matrix nano-composites (HAlMMNCs)[3)]. The lightweight structures and automotive components were the uses of such advanced aluminum-based composites in different corroding environments. The corrosion investigation is a significant parameter for accessing potential applications of hybrid composites to structural and component manufacturing in various industries[4)].

A lot of research was carried out on the physical, mechanical, and tribological behavior of AlMMNCs, however, the study of corrosion behavior as metallurgical characteristics has to be explored so far. The corrosion may be accelerated due to the interaction of reinforcement particles with matrix material in physical, chemical, and electrochemical forms[5–7)]. The galvanic interaction of reinforcement and matrix also causes to increase in material loss and corrosion of the composite. The rapid penetration of reinforcement and matrix caused preferential corrosion along the interfacial region in MMCs. These difficulties can be prevented in AlMMNCs compared to monolithic alloys and enhance the corrosion resistance of fabricated AlMMNCs[8)]. The cracks, pit holes, and inhomogeneities can be arises in the composites, which tends to result in a decrement in load-bearing capacity and catastrophic failure of the material. These defects present in composites limits the application in a corrosive environment under the existence of stress[9)].

The previous findings focused on pitting potential and excavation morphology when performing corrosion tests in exposure to Nacl solution[10)]. Authors also observed crater and holes initiates due to reinforcements in the matrix and this could be the reason for pits generation in the composites compared to monolithic alloys[11)]. Baig et.al. concluded that the low volume fraction of Al_2O_3 as

reinforcement increases the corrosion resistance of MMCs[12]. The di-anodic reaction method was used for the improvement of corrosion resistance by Anaee et al[13]. The corrosion occurred at two regions of the composite materials; a region next to the intermetallic area and a dendritic structure around the pitting region. There was no galvanic corrosion happens between the SiC and Al-matrix. Further pitting potential was not affected by reinforcement particulates in fabrication of AlMMCs using stir casting process[14]. The current study investigates the corrosion behavior of Al-cerium oxide (CeO_2) MMCs immersed in (1 – 3.5 wt.%) NaCl and H_2So_4 solution at elevated and ambient temperatures. The composite of Al-CeO_2 was prepared using stir casting route reinforced with (1-3 wt.%) of CeO_2 as rare earth particulates (REPs). The influence of REPs nano size and weight percentage on the corrosion characteristics was broadly examined.

2. Material and methods

The aluminum alloy 6061 was used as raw material reinforced with nano CeO_2 in 1, 2, and 3 weight percentage thru stir casting technique. The Al-6061 was received plate form having size of 150 mm x 50 mm x 10 mm and this was converted into 30 mm x 20 mm x 10 mm. The composition was tested and constituents were mentioned in table1. The CeO_2 nanoparticle was used as reinforcement with 99.9 % purity level and 2 to 4 nm in size as provided by NRL (Nano Research laboratory) Jamshedpur-INDIA. The 3670 ºC and 2.3 g/cm^3 were the melting temperature and density of the REPs, respectively.

The monolithic alloy was prepared into ingots 30 mm x 20 mm x 10 mm using power hacksaw and then superheated in an electric furnace at 820 °C. To remove the moisture contents from the nano CeO_2, the nano-filler was preheated at 300 °C. The Al-6061 alloy was converted into molten metal at superheating temperature and then furnace temperature was maintained at 750 °C. The vortex was created with help of diamond coated stirrer. After obtaining the appropriate vortex, the reinforcement percentage was added in the liquid pool and stirring action was done at 300 rpm for 10 minutes. To ensure proper dispersion, the stirring speed was increased and decreased between 300 to 200 rpm respectively for 10 minutes. To enhance the wettability, 2 % magnesium powder was added in the molten metal. After proper mixing of reinforcement and magnesium in the liquid pool then pouring was done in steel mould and allowed to cool at room temperature. The casted samples were withdrawn from the steel mould carefully and prepare the samples for testing. The metallurgical behavior of the casted and corroded specimens was examined with the help of scanning electron microscopy (SEM) present in IIC Centre (Physics department), NIT, Kurukshetra.

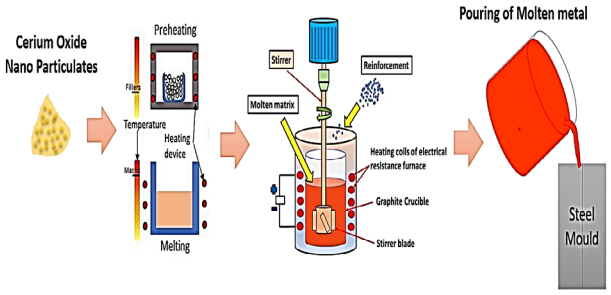

Figure 1: Graphical form of Stir cast Al-CeO_2 nano-composite process

3. Characterization and testing

3.1 Density

Before testing the density of the specimens, they were grounded on abrasive rotating discs of grit size up to 1500 underwater. Then the polishing was done with 2 µm Al_2O_3 paste and after that, the specimens were cleaned using acetone[15]. The Archimedes principle was used to calculate the density of the prepared specimens. The ASTM B311-08 standard was followed to investigate the density of AlMMNCs[16]. The rule of the mixture was utilized for calculating the theoretical densities of the AlMMNCs specimens. The round-shaped specimens were weighed one by one in the air (wa), then submerged under de-ionized water and weighed again (wd). The experimental density was calculated using the equation (1):

$$\rho_e = \frac{w_a}{(w_a - w_d)} x\, \rho_d \qquad (1)$$

Where experimental density was denoted by ρ_e, w_a and w_d are the weights of specimens in air and under de-ionized water in grams. The density of the de-ionized water was denoted by ρ_d. The digital weighing machine with an accuracy of 10^{-4} grams was used for the weight measurement of the specimens.

3.2 Corrosion test

The corrosion test was carried out at three temperatures, characteristically, ambient temperatures, 45, and 75 ºC under static conditions. The mass loss was observed to measure the corrosion rate of stir-cast Al-CeO_2 nano-composite using the digital weighing machine. The specimens were weighed before and after immersion in NaCl and H_2So_4 solutions. Three replicates for each sample were used for each corrosion test to get the mean value of corrosion rate. The total duration of the specimen's immersion in solutions is 180 hours. The weight of the specimen after immersion was measured after a time interval of 36 hours, for example (the immersed weight of the specimen after drying later on at

36, 72, 108, 144, and 180 hours respectively). The mass loss of the specimens was then transformed into corrosion rate which was stated in terms of mm penetration per year. The SEM analysis was done of the corroded AlMMNCs surfaces. The 2.5 wt.% static aqueous solutions of NaCl and H_2So_4 were used for corrosion tests. In order to prevent crevice corrosion, a plastic string was wound on the AlMMNCs specimen and then immersed in the solutions. The ASTM G31 standard was followed to evaluate the corrosion rate by use of mass loss measurement. The 20 x 20 x 5 mm specimen size was prepared for corrosion test. The Al-CeO_2 nano-composite specimens were ground to 1500 grits on abrasive discs and then cleaned with de-ionized water and methanol, dried afterward, and then immersed in the aqueous solutions of NaCl and H_2So_4.

The electric heater was used to prepare the NaCl and H_2So_4 solution for the accelerated test or to obtain the elevated temperature of the solutions for corrosion tests. The aqueous solutions were heated to 45 ± 5 ºC and 75 ± 5 ºC after that the specimens were immersed in the heated solutions and covered the vessel with glass to avoid evaporation. From the mass loss, the corrosion rate (COR) was examined with the use of equation (2) as mentioned below:

$$COR = \frac{Q \times M}{a \times \rho \times E_t} \qquad (2)$$

Where corrosion rate is denoted by COR in (mm/year), Q is constant (8.766 x 10^4), M as mass loss in (mg), a is the area of the specimen in cm^2, the ρ is the density of the specimen in (g/cm^3), and E_t is exposure time in (hours) to the nearest value of 0.01 hours.

4. Results and discussion

4.1. Density of AlMMNCs

Figure 2 shows the experimental values of densities of fabricated AlMMNCs with different weight percentages of nano-size REPs. The lower densities were observed in the AlMMNCs compared to Al-6061 alloy. The AlMMNCs revealed experimental densities of about 98-99% of the theoretical densities. The 2.704, 2.698, and 2.695 g/cm^3 were noticed as densities of Al-CeO_2 nano-composite reinforced in 1, 2, and 3 wt. %, respectively. The as-casted Al-6061 alloy has a density of 2.71 g/cm^3. The increase of CeO_2 % weight decreases the density of the AlMMNCs samples. The results indicate that a reduction of densities is observed at a rate of strengthening of AlMMNCs. The effective density 2.5304 g/cm^3 was observed in as-cast Al-8090 alloys, while a lower value 2.5120 g/cm^3 of density was found in the Al-8090/2-percent SiC/6-percent B_4C alloys in HAMMCs[17].

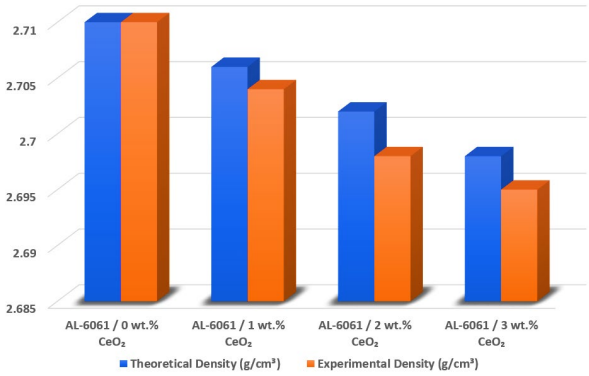

Figure 2: Shows the densities AlMMNCs reinforced with different wt.%

The increasing percentage weights from the grain-refiners and modification in the LM25 alloy increased the density of composite materials [18]. Jatinder Kumar et.al produced the stir cast AMCs reinforced with silicon carbide (SiC) and molybdenum (Mo). The results revealed that the densities of the fabricated samples were enhanced with volume percent of the reinforcements in the AMCs samples [19]. Following the trends of previous findings, the higher densities of reinforcement results in the increment of densities for fabricated MMCs[19s–21]. However, the cerium oxide has low density compared to Al-6061 alloy, so the fabricated AlMMNCs samples possess low densities compared to monolithic alloy.

4.2 Microstructural characteristics of stir-casted AlMMNCs

Figure 3 (a-d) shows the SEM analysis of AlMMNCs with CeO_2 at 0, 1, 2, and 3 wt.%. some defects were observed after the stir casting in the composite material. The presence of CeO_2 was shown as white region in figure 3 (b-d). Figure 3 (a) shows deformation on the surface of as-casted Al-6061 alloy. Figure 3 (b) represents some voids and inhomogeneities of the REPs in Al-6061 alloy. Some

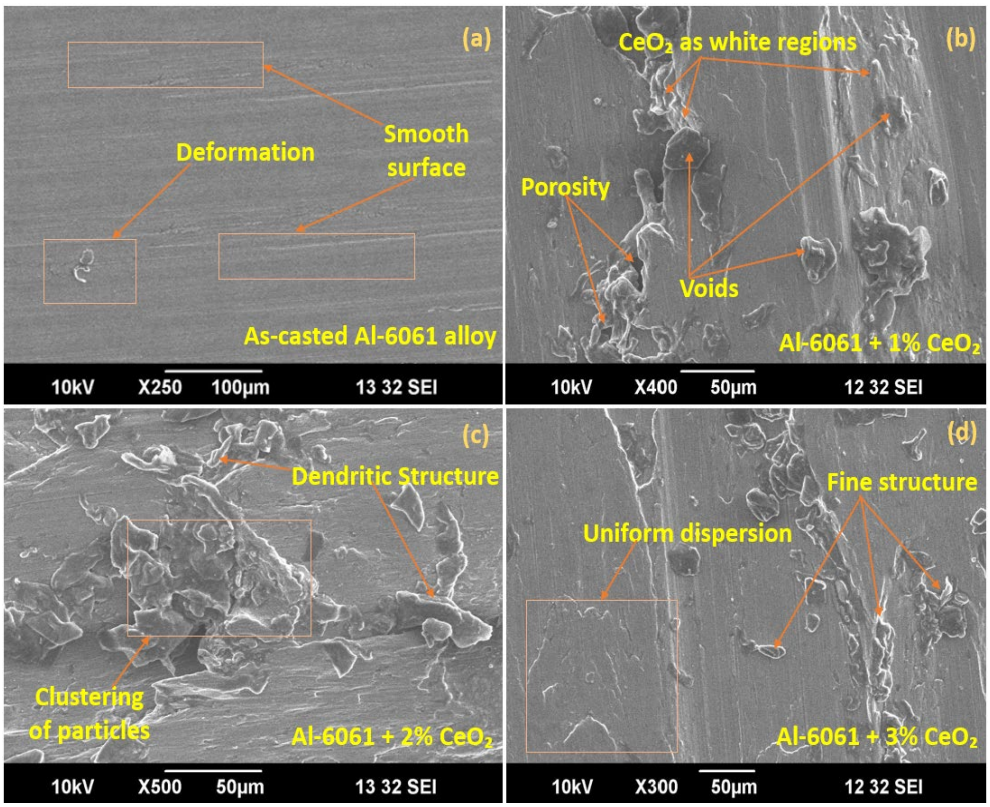

Figure 3 (a-d): SEM analysis of AlMMNCs with CeO_2 at (0-3) wt.%

dentritics structures and clustreing of particles were noticed in figure (c). The proper mixing of reinforcement in the matrix material and fine grain refinement were observed in figure 3(d). The nano reinforcement enhances the densities of the AlMMNCs samples. The uniform dispersion led to enhancing the mechanical and metallurgical properties of the fabricated samples. The enhancement in the mechanical was directly proportional to the increment in the weight fraction of the prepared specimens [23,24]. Shuvho et al. observed the microstructure behavior of the aluminum hybrid metal matrix composites with Al_2O_3, TiO_2, and SiC as reinforcement. The casting defects such as; voids, cracks, agglomeration of reinforcement particles and porosity were observed in the microstructure images[25,26].

The microstructural investigation of AMMCs reinforced with carbon nanotubes (CNT), Al_2O_3, and SiO_2 in Al-matrix was done. The nearly identical grain size of the Al_2O_3 and CNT reinforced composite were observed from SEM images. The AMMC sample with pure aluminum gave the effective particle grain size fabricated with spark plasma sintering. The coarser SiO_2 particles present in AMMCs possess less grain refinement as compared to other composites reinforced with CNT and Al_2O_3. The addition of ceramic particles below the particular dimension of particles results in enhancement of grain refinement. The mean grain refinement size of 14 and 10 µm were measure in Al_2O_3 and CNT reinforcements, respectively, however the 34 µm mean grain refinement size was observed with SiO_2 reinforced in fabricated composites. In addition to the grain refinement, the vibrant bi-modal structure arises with coarse grainsize of SiO_2 and supplementary equiangular microstructure was produced due to Al_2O_3 and CNT reinforcements in AMMCs[27]. Daly et al. fabricated the Al-Sic MMC using stir casting method. The evaluation of microstructural characteristics was done with SEM images. The development of good interface between the matrix and reinforced material was observed after the SEM analysis. There is no porosity was found in the fabricated composite when we analysis up to nano-scaled level. The author also confirms the proper wettability and uniform distribution of particles in the composites due to finest size of the crystals of aluminum and silicon carbide in AMMCs. The mechanical properties were also enhanced in the fabricated composites, which confirms the strong interface developed in the AMMCs samples[28,29]. The homogenous dispersion was noticed with Sic particles in aluminum matrix composite. The excellent and uniform dispersion of reinforcement particles also enhanced the mechanical and physical properties of the composite. The higher the weight percentage of Sic nanofiller in aluminum displays the improved dispersion of matrix and reinforcement particles without agglomeration of the particles in fabricated Al-SiC composites[30].

4.3. Corrosion behavior of AlMMNCs

Figure 4 (a and b) represent the variation in the

corrosion rate of AlMMNCs samples under 2.5 wt.% NaCl and H_2So_4 solutions at ambient temperature with exposure time. The AMMCs reinforced with wt.% of CeO_2 exhibited better corrosion resistance compared to monolithic Al-6061 alloy during the immersion test for both the aqueous solutions. So, it has been noticed that the corrosion resistance was enhanced with an increment in the weight percentage of the reinforcements. The nano-size of the reinforcement was also found significant in reducing the corrosion rate of the AlMMNCs. However, it has also been observed during the corrosion test of the Al-6061 alloy that the corrosion resistance decreased with the increment in exposure time. Now the phenomenon of decrement in corrosion resistance with an increase in exposure time has been changed in AMMCs specimen which indicates the anodic stabilization of AlMMNCs. The corrosion behavior of Al-B_4C metal matrix composite was carried out in 3.15 wt.% of NaCl solution. The study concluded that after the immersion test, some defects were created on subsurface of the composite specimen. The lower oxidation rate was observed in Al-B_4C specimens compared to aluminum alloy[8]. Similarly, the polarization behavior of Al- B_4C was evaluated in 0.5 M Na_2SO_4 solution. The B_4C reinforced AMMCs samples found 10% higher corrosion resistance compared to monolithic Al-alloy[8]. Liaqat Ali Shah et al. analyze the corrosion resistance of Al-based MMCs reinforced with TiB_2 particles using Tafel polarization in 3.5 wt.% NaCl solution. The increment in corrosion resistance was recorded as the reinforcement wt.% is increased in AMMCs [31]. The comparative analysis of corrosion in Al-Al_2O_3 and Al-SiC MMCs using anodization and immersion test in cerium oxide[32]. The surface treatment enhanced the corrosion resistance in both the MMCs, but Al_2O_3 particles achieved better corrosion resistance compared to SiC particles. However, the low pitting corrosion was also observed in Al-Al_2O_3 samples compared to Al-SiC MMCs[33]. Singh et. al. fabricated the MMC of Al-Cr using stir casting technique and analyzed the corrosion behavior on fabricated AMMCs samples. The electrochemical impedance spectroscopy technique had utilized in the presence of 0.5M H_2SO_4 solution for corrosion characteristics of the developed MMCs. The corrosion rate was enhanced by reinforcing the Cr particle to the pure Al-alloy. Further, corrosion resistance comparison had also made between MMCs reinforced with nano and micro-Cr particle to Al matrix. The anti-corrosion potential quality of Cr particles in matrix material enhances the corrosion resistance characteristic in the fabricated composites[34]. The MMCs with nano-particle filler shows the better corrosion resistance compared to micro-filler particles. In general terms, the Cr with nano-filler has advanced shielding phenomenon under corroded environment compared to monolithic Al-alloys as well as micro -filler reinforcement MMCs[35]. Following the same trends, the current study observed the intermetallic due to reaction results of Al-6061 and CeO_2 particulates. Thus, an optimistic advantage can be seen in the corrosion resistance of the prepared composite due to the discontinuity of aluminum matrix alloy or the addition of nano CeO_2 in the matrix material in the stir casting process. Furthermore, the decrement was recorded in mass loss of the ALMMNCs in static 2.5 wt.% of NaCl and H_2So_4 solutions with a decrement in particle size or nano -size.

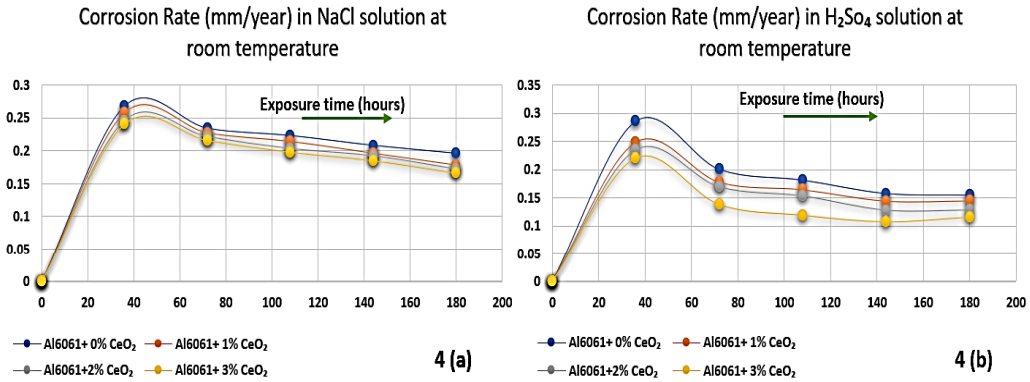

Figure 4 (a and b): COR of AlMMNCs samples at room temperature in aqueous solutions

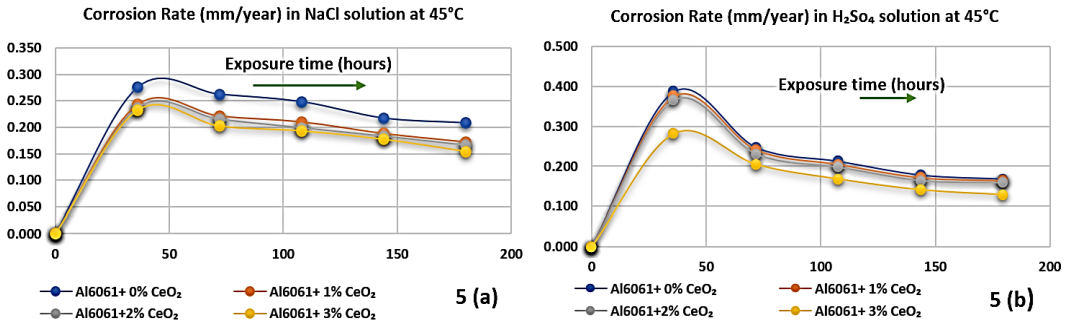

Figure 5 (a and b): COR of AlMMNCs samples at 45 °C in aqueous solutions

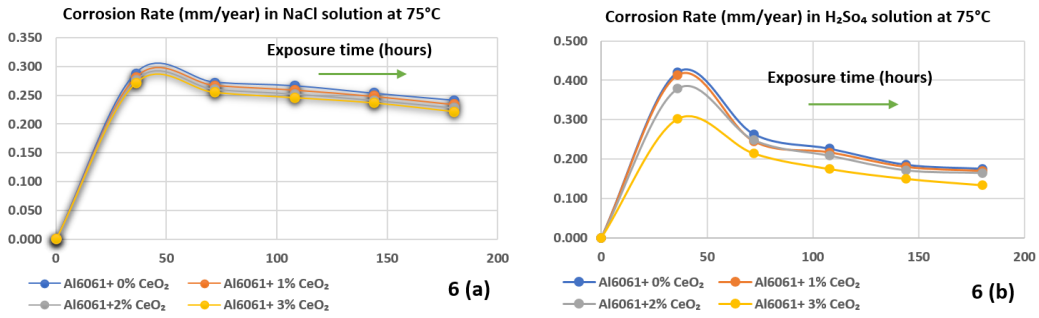

Figure 6 (a and b): COR of AlMMNCs samples at 75°C in aqueous solutions

Figures 5 (a and b) and 6 (a and b) show the corrosion rate variation of AlMMNCs specimens after exposure of 36 to 180 hours, immersed in 2.5 wt.% of NaCl and H_2So_4 solutions, at 45 and 75 °C respectively. The results of the immersion test at room and elevated temperature show that a higher corrosion rate was achieved with H_2So_4 solutions compared to NaCl. However, results compared to the matrix material, a lower corrosion rate was observed in AlMMNCs compared to monolithic alloy. The decrement in the corrosion rate was noted with an increment in the weight percentage of the CeO_2 particulates in prepared AlMMNCs. A linear increment was noticed in the corrosion rate as exposure time and the temperatures were increased during immersion testing of fabricated composites.

4.4 Morphology of corroded AlMMNCs surface

The corroded surfaces of Al-6061 alloy and AlMMNCs reinforced with 1-3 wt.% of Cerium oxide were represented in figure 7 (a, b, c, and d) after SEM analysis. The immersion test was performed under 2.5 wt.% of NaCl and H_2So_4 solutions after 36 h, 72h, and 180h as exposure time at room temperature, 45°C, and 75°C. Severe damage was found on Al-6061 and AlMMNCs surfaces. The large pitting defects in the NaCl medium were produced on the Al-6061 surface as shown in figure 7(a) and were seen by physical examination also. However, Al-CeO_2 composite with 3 wt.% of reinforcement exhibits a reduced amount of damage under NaCl solution compared to the monolithic matrix material as shown in figure 7(b). The cracks and pitting corrosion behavior was noticed in AlMMNCs specimen under NaCl solution at room temperature after 72 hours of exposure time. Figure 7(c) represents the severe degradation on the surfaces of AlMMNCs specimen reinforced with 3 wt.% in an H_2So_4 medium at room temperature after 72 hours of exposure time. After 72 hours of exposure time the corrosion behavior was noticed as cracks, voids and dimples in the AlMMNCs specimen as confirmed by SEM analysis. The clustering of reinforcement particles was seen in AlMMNCs specimens in H_2So_4 solution at 75°C after 72 hours of exposure time as represented in figure 7(d). This is because of disturbed grain boundaries and results in microstructural changes as the corrosion effect. In addition to clustering, pitting defects also occurred due to the non-uniform distribution of reinforcement particles. Magnified SEM micrographs also confirm the pitting behavior in the agglomerated region of the fabricated AlMMNCs. The corrosion rate was more affected by H_2So_4 solution compared to NaCl at elevated temperature of 75°C. The CeO_2 as rare earth oxide remains slugged into matrix material during immersion in NaCl solution and being less anodic, was the reason for being more corrosion resistive than immersed in H_2So_4 medium. Although, fewer pits were observed with increment in the addition of nano-sized REPs in the Al-6061 alloy. The investigation also confirms the formation of grain boundary corrosion in fabricated nanocomposite as shown in figure 7(d). The reinforcement particles restrain this behavior to a certain limit with increment in addition of CeO_2 particulates but cannot be able to eliminate.

Figures (4, 5, and 6) also shows that the surface

degradation is higher with heated aqueous solutions for both pure Al-6061 alloy and nano AlMMCs. However, AlMMNCs possess higher corrosion resistance compared to the monolithic matrix alloy with an increase in the exposure period. The size and number of pits in per unit area were observed for incremented temperature and immersion in 2.5 wt.% of NaCl and H_2So_4 solutions. The corrosion behavior of AlMMNCs influenced by several aspects; processing methods; kind and characteristics of matrix materials; shape, size, weight / volume percentage of reinforcements; type of corrosive solutions, and environmental circumstances[36]. Dogan Semsek performed the corrosion test in NaCl and H_2So_4 solution for AMCs reinforced with ZrO_2 and graphite. The pitting and fretting corrosion were observed as main degradation effect on the surfaces during tests. The NaCl solution was found to be better corrosion resistance compared to H_2So_4 solution[37]. The influence of corrosion in Al-SiC MMCs led to development of interphases between aluminum and silicon carbide, which causes voids and cracks on the MMCs surface[3]. Sunday Aribo et. al. prepared stir cast composite of Al6063 reinforced with SiC and snail-shell-Ash (SSA) and performed the corrosion tests. The results revealed that increment in the reinforcement percentage increases the hardness of the MMCs. The higher the hardness of the MMCs led to enhancement in corrosive resistance of the hybrid MMC samples[38]. Bodunrin et. al. investigated the influence of corrosion behavior of Al-6063/SiC_p MMCs in 0.3M H_2So_4 and 2.5 wt.% of NaCl solutions. The SiC_p presence in the aluminum alloy gives the superior corrosion resistance in NaCl solution compared to H_2So_4. Furthermore, the corrosion resistance was significantly enhanced with thermomechanical treatment of the MMCs in H_2So_4 solution[39]. In current study, the interfacing of matrix and reinforcements plays the vital role in fabrication of AlMMNCs samples. Stronger the interfacial bonding, higher the corrosion resistance capability of the produced hybrid nanocomposite. The improvement corrosive resistance was noticed in Al-6061-3wt.% CeO_2 HMMCs which is the consequence of strong interfacial bonding and uniform distribution of matrix and reinforcement particulates in the AlMMNCs.

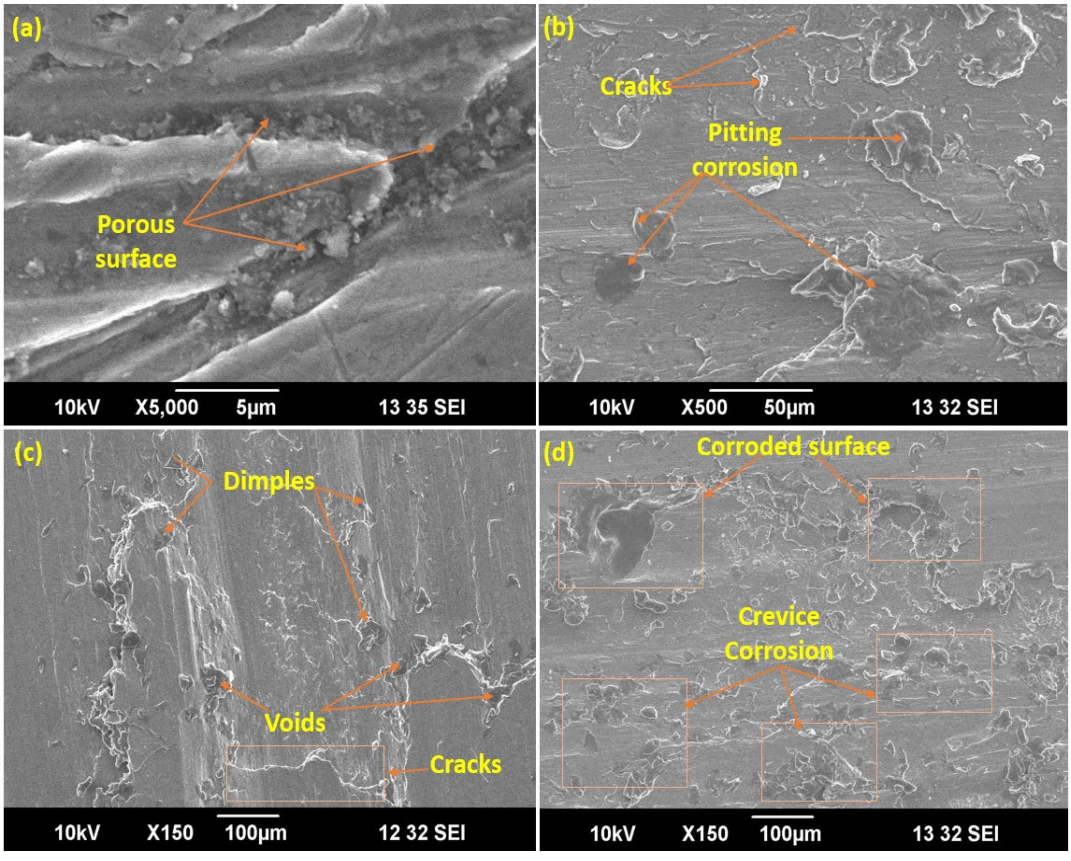

Figure 7 (a-d): (a) Corroded surfaces of Al-6061 alloy immersed in NaCl solution at room temperature, **(b)** Corroded surfaces of Al-6061/3wt.% CeO_2 immersed in NaCl solution at room temperature after 72 h exposure time, **(c)** Corroded surfaces of Al-6061/3wt.% CeO_2 immersed in H_2So_4 solution at room temperature after 72 h exposure time, **(d)** Corroded surfaces of Al-6061/3wt.% CeO_2 immersed in H_2So_4 solution at 75°C after 72 h exposure time.

4.5 Mechanism controlling the corrosion Behavior

The primary factor for the occurrence of corrosion in the material is in the form of pitting corrosion. Initiation, propagation, and perforation are the three stages in pitting corrosion which ultimately led to formation of dimples, cracks, and voids in the composite surfaces[37]. The second factor was fretting corrosion, which produces the corroded surfaces and material loss in the MMCs[40]. The pitting and fretting corrosion can be prevented by adopting good design of the component. Reinforcement particles like SiO_2, Al_2O_3, SiC and CeO_2 decreases corrosion rates in AlMMCs, but corrosion rates are increased in high temperatures as compared with monolithic alloys[41–43]. However, the improvement of corrosion resistance was observed in AlMMNCs when the addition of nano-sized reinforcement particles was made to the monolithic alloy [44–46]. The sample should have less stress concentration under controlled environmental condition[47]. The less bends and tensile stress in the sample reduces stress concentration in the component and avoiding chloride solution gives better and healthy environment and thus reduces the corrosion rate of the AlMMCs[48]. Another behavior of corrosion was in the form of erosion of the material, which causes due to electrochemical action of the aqueous solution[49]. The erosion can be prevented by making the material erosion resistant. The easy draining and cleaning of the components can make the material more erosion resistant[50]. The energy activation of matrix and reinforcement particulates also leads to corrosion which causes due to immersion in heated aqueous solution. The corrosion was occurring in the form of thermal softening and melting of the material[51]. Higher the energy activation, higher will be the corrosion rate in the AlMMNCs[52]. The electroplating and coating mechanism on composite surface with non-corrosive material reduces the chance of energy activation in the presence of heated aqueous solutions[53]. This can be concluded that these mechanisms can minimize and prevent the corrosion rate up to an extent but could not eliminate completely in the AlMMNCs surface under serve environmental conditions.

5. Conclusions

The following conclusions are drawn after analyzing the results as mentioned below:

- The as-cast and nanocomposite samples has been fabricated with (1 to 3) wt.% of CeO_2 using the stir casting technique.
- The corrosion behavior of Al-6061 alloy (unreinforced) and AlMMNCs (reinforced with CeO_2) has been observed at different temperatures (room temperature, 45ºC, and 75ºC) and exposure time (36-180 hours) in 2.5 wt.% of NaCl and H_2So_4 solutions.
- The lower corrosion resistance was observed in fabricated AlMMNCs samples compared to monolithic alloy (Al-6061) under all parametric conditions.
- The increment in the reinforcement increases the corrosion resistance of the prepared nanocomposites. The nano-sized reinforcement particulates in addition to increment in exposure time and temperature of the aqueous solutions also decreases the corrosion rate of the AlMMNCs.
- The 0.116 has been observed as significant corrosion rate in mm potential per year after 180 hours as exposure time at 75ºC in 2.5 wt.% NaCl solution. The intermetallic bonding of the reinforcement with matrix material is the reason for this enhancement of corrosivity of the prepared aluminum nanocomposites with 3 wt.% CeO_2.
- The electroplating and coating of anti-corrosive materials, less energy activation and anodic reaction were the controlling mechanism for the prevention of corrosion behavior in AlMMNCs.

References

1) D. Kumar, S. Angra, and S. Singh, “Mechanical properties and wear behaviour of stir cast aluminum metal matrix composite: a review,” *Int J Eng Trans A Basics*, **35** (*4*) 794–801 (2022). doi:10.5829/IJE.2022.35.04A.19.
2) D. Kumar, S. Singh, and S. Angra, “Effect of reinforcements on mechanical and tribological behavior of magnesium-based composites : a review,” **50** (*3*) 439–458 (2022). doi:10.18149/MPM.5032022.
3) S.P. Dwivedi, S.P. Dwivedi, M. Maurya, and S.S. Chauhan, “Mechanical , physical and thermal behaviour of sic and mgo reinforced aluminium based composite material mechanical , physical and thermal behaviour of sic and mgo reinforced aluminium based composite material,” Evergreen,**8** (*2*) 318–327 (2021).
4) S. Rajkumar, S. Loganathan, R. Venkatesh, and B.S. Madhan Prabhu Deva, “Investigate of wear behaviour and mechanical properties of titanium diboride reinforced ammc composites,” *J New Mater Electrochem Syst*, **24** (*4*) 254–260 (2021). doi:10.14447/jnmes.v24i4.a04.
5) A.K. Chanda, A. Kumar, A.K. Chanda, and S. Angra, “Optimization of stiffness properties of composite sandwich using hybrid taguchi-gra-pca optimization of stiffness properties of composite sandwich using hybrid taguchi-gra-pca,” Evergreen,**8** (*2*) 310–317 (2021).
6) A.K. Chanda, A. Kumar, A.K. Chanda, and S. Angra, “Numerical modelling of a composite sandwich structure having non metallic honeycomb core numerical modelling of a composite sandwich structure having non metallic honeycomb core,” Evergreen,**8** (*4*) 759–767 (2021).
7) D. Kumar, S. Singh, and S. Angra, “Dry sliding wear and microstructural behavior of stir-cast al6061-based composite reinforced with cerium oxide and graphene nanoplatelets,” *Wear*, **516**–**517** (*September*

2022) 204615 (2023). doi:10.1016/j.wear.2022.204615.

8) H. Ding, and L.H. Hihara, "Electrochemical examinations on the corrosion behavior of boron carbide reinforced aluminum-matrix composites," *J Electrochem Soc*, **158** (*5*) C118 (2011). doi:10.1149/1.3567519.
9) P.P. Kumari, and S. Kagatikar, "Mannich base as an efficient corrosion inhibitor of aa6061 in 0 . 5 m hcl : electrochemical , surface morphological and theoretical investigations," *Arab J Sci Eng*, **47** (*6*) 7053–7067 (2022). doi:10.1007/s13369-021-06302-2.
10) N. Munasir, Triwikantoro, M. Zainuri, R. Bäßler, and Darminto, "Corrosion polarization behavior of al-sio2 composites in 1m and related microstructural analysis," *Int J Eng Trans A Basics*, **32** (*7*) 982–990 (2019). doi:10.5829/ije.2019.32.07a.11.
11) T.M. Harish, S. Mathai, J. Cherian, K.M. Mathew, T. Thomas, K. V. Vishnu Prasad, and V.C. Ravi, "Development of aluminium 5056/sic/bagasse ash hybrid composites using stir casting method," *Mater Today Proc*, **27** (*xxxx*) 2635–2639 (2019). doi:10.1016/j.matpr.2019.11.081.
12) M.M.A.B.A.M. Al, Q.I.M. Allam, F. Patel, and A. Samad, "Tribological performance of sub - micron - al 2 o 3 - reinforced aluminum composite brake rotor material," *Arab J Sci Eng*, **46** (*3*) 2691–2700 (2021). doi:10.1007/s13369-020-05179-x.
13) R.A.M. Anaee, "Study of corrosion behavior of al-si-cu / wc composites in 0 . 1 n naoh solution," **26** (*1*) 55–65 (2015). doi:10.4197/Eng.
14) A.S.F.Y.M. Abdallah, "Corrosion inhibition of aluminum – silicon alloy in 1 m hcl solution using phenazone and aminophenazone," 5363–5371 (2014). doi:10.1007/s13369-013-0824-6.
15) V.K. Mittal, "Experimental investigation for tribological properties in mixed regime of lubrication with experimental investigation for tribological properties in mixed," Evergreen,**9** (*3*) 694–700 (2022).
16) D. Choudhari, "Characterization and analysis of mechanical properties of short carbon fiber reinforced polyamide66 composites characterization and analysis of mechanical properties of short carbon fiber reinforced polyamide66 composites," Evergreen,**8** (*4*) 768–776 (2021).
17) R. Leo Bright Singh, G.R. Jinu, M. Manoj, and A. Elaya Perumal, "Tribological behaviour of al8090-sic metal matrix composites with dissimilar b4c addition," *Silicon*, (*0123456789*) (2022). doi:10.1007/s12633-021-01608-0.
18) R. Tamuly, A. Behl, and H. Borkar, "Effect of addition of grain refiner and modifier on microstructural and mechanical properties of squeeze cast a356 alloy," *Trans Indian Inst Met*, (2022). doi:10.1007/s12666-022-02607-4.
19) J. Kumar, D. Singh, N.S. Kalsi, S. Sharma, M. Mia, J. Singh, M.A. Rahman, A.M. Khan, and K.V. Rao, "Investigation on the mechanical, tribological, morphological and machinability behavior of stir-casted al/sic/mo reinforced mmcs," *J Mater Res Technol*, **12** 930–946 (2021). doi:10.1016/j.jmrt.2021.03.034.
20) A.C. Opia, M. Kameil, A. Hamid, C.A.N. Johnson, W. Reduction, A.C. Opia, M. Kameil, A. Hamid, C.A.N. Johnson, A.B. Rahim, and M.B. Abdulrahman, "Nano-particles additives as a promising trend in tribology : a review on their fundamentals and mechanisms on friction and wear reduction nano-particles additives as a promising trend in tribology : a review on their fundamentals and mechanisms on frictio," Evergreen,**8** (*4*) 777–798 (2021).
21) "An overview of recent development and application of friction stir processing technique an overview of recent development and application of friction stir processing technique," Evergreen,**9** (*3*) 814–829 (2022).
22) S.H. Ador, S. Kabir, F. Ahmed, F. Ahmad, and S. Adil, "Effects of minimum quantity lubrication (mql) on surface roughness in milling al alloy 383 / adc 12 using nano hybrid cutting fluid," Evergreen,**09** (*04*) 1003-1020 (2022).
23) A. Nojima, A. Sano, H. Kitamura, and S. Okada, "Electrochemical characterization , structural evolution , and thermal stability of livopo _ 4 over multiple lithium intercalations electrochemical characterization , structural evolution , and thermal stability of livopo 4 over multiple lithium," Evergreen,**6** (*4*) 267–274 (2019).
24) S.P. Dwivedi, S.P. Dwivedi, N.K. Maurya, and M. Maurya, "Assessment of hardness on aa2014 / eggshell composite produced via electromagnetic stir casting method assessment of hardness on aa2014 / eggshell composite produced via electromagnetic stir casting method," Evergreen,**6** (*4*) 285–294 (2019).
25) M.B.A. Shuvho, M.A. Chowdhury, M. Kchaou, A. Rahman, and M.A. Islam, "Surface characterization and mechanical behavior of aluminum based metal matrix composite reinforced with nano al2o3, sic, tio2 particles," *Chem Data Collect*, **28** 100442 (2020). doi:10.1016/j.cdc.2020.100442.
26) "Effectiveness analysis of ozonation for prevention of corrosion and precipitation of crust in closed system cooling towers effectiveness analysis of ozonation for prevention of corrosion and precipitation of crust in closed system cooling towers," Evergreen,**8** (*4*) 904–909 (2021).
27) B. Sadeghi, P. Cavaliere, and A. Perrone, "Effect of al2o3, sio2 and carbon nanotubes on the microstructural and mechanical behavior of spark plasma sintered aluminum based nanocomposites," *Part Sci Technol*, **38** (*1*) 7–14 (2020). doi:10.1080/02726351.2018.1457109.

28) A.A. El-Daly, M. Abdelhameed, M. Hashish, and W.M. Daoush, "Fabrication of silicon carbide reinforced aluminum matrix nanocomposites and characterization of its mechanical properties using non-destructive technique," *Mater Sci Eng A*, **559** 384–393 (2013). doi:10.1016/j.msea.2012.08.114.
29) G.A. Strategy, "Experimental & analytical investigation for optimization of disc brake heat dissipation using cfd," Evergreen,**09** (*04*) 1076-1089 (2022).
30) A.P. Rath, S.K. Patel, and N. Deep, "Synthesis and characterisation of silicon carbide nanoparticulate reinforced metal matrix composite," *Mater Today Proc*, **33** (*xxxx*) 5419–5424 (2020). doi:10.1016/j.matpr.2020.03.136.
31) L.A. Shah, "Thermodynamic prediction and synthesis of a titanium diboride powder by reduction of titanium dioxide with boron carbide in argon atmosphere," *Arab J Sci Eng*, **47** (*6*) 7551–7558 (2022). doi:10.1007/s13369-021-06213-2.
32) C. Cui, M. Wu, X. Miao, Z. Zhao, and Y. Gong, "Microstructure and corrosion behavior of ceo2/feconicrmo high-entropy alloy coating prepared by laser cladding," *J Alloys Compd*, **890** 161826 (2021). doi:10.1016/j.jallcom.2021.161826.
33) M. Sambathkumar, R. Gukendran, and M. Vijayanand, "Materials today : proceedings investigation of corrosion behaviour of al 7075 / b 4 c / al 2 o 3 hybrid metal matrix composite," *Mater Today Proc*, **50** 1606–1610 (2022). doi:10.1016/j.matpr.2021.09.123.
34) T.O. Joshua, K.K. Alaneme, M.O. Bodunrin, and J.A. Omotoyinbo, "Corrosion and wear characteristics of al-zn based composites reinforced with martensitic stainless steel and silicon carbide particulates," *Mater Today Proc*, **62** (*xxxx*) S127–S132 (2022). doi:10.1016/j.matpr.2022.02.099.
35) M. Kanyathia, "Influence of chromium with rare earth oxide addition on microstructure and corrosion resistance of grey cast iron hard facing alloy .," **13** (*9*) 105–111 (2018).
36) P. Sureshkumar, T. Jagadeesha, L. Natrayan, M. Ravichandran, D. Veeman, and S.M. Muthu, "Electrochemical corrosion and tribological behaviour of aa6063 / si 3 n 4 / cu (no 3) 2 composite processed using single-pass ecap a route with 120 die angle," *J Mater Res Technol*, **16** 715–733 (2021). doi:10.1016/j.jmrt.2021.12.020.
37) D. Şimşek, D. Özyürek, and S. Salman, "Wear behaviors at different temperatures of zro2 reinforced a356 matrix composites produced by mechanical alloying method," *Ind Lubr Tribol*, **74** (*5*) 463–471 (2022). doi:10.1108/ILT-10-2021-0416.
38) S. Aribo, A. Fakorede, O. Ige, and P. Olubambi, "Erosion-corrosion behaviour of aluminum alloy 6063 hybrid composite," **377** 608–614 (2017).
39) M.O. Bodunrin, K.K. Alaneme, and S.J. Olusegun, "Influence of thermomechanical processing on the corrosion behaviour of aluminium (6063) -sic p composites in nacl and h 2 so 4 environment," **2** (*2*) 17–25 (2011).
40) S. Banerjee, S. Poria, G. Sutradhar, and P. Sahoo, "Corrosion behavior of az31-wc nano-composites," *J Magnes Alloy*, **7** (*4*) 681–695 (2019). doi:10.1016/j.jma.2019.07.004.
41) A. Cu, and S. Hybrid, "Characterization of stir cast al cu (fly ash + sic) hybrid metal matrix composites," **44** (*8*) (2010). doi:10.1177/ 0021998309346386.
42) H.C.A. Murthy, V.B. Raju, and C. Shivakumara, "Effect of tin particulate reinforcement on corrosive behaviour of aluminium 6061 composites in chloride medium," **36** (*6*) 1057–1066 (2013).
43) K. Kamal Babu, K. Panneerselvam, P. Sathiya, A. Noorul Haq, S. Sundarrajan, P. Mastanaiah, and C. V. Srinivasa Murthy, "Parameter optimization of friction stir welding of cryorolled aa2219 alloy using artificial neural network modeling with genetic algorithm," *Int J Adv Manuf Technol*, **94** (*9–12*) 3117–3129 (2018). doi:10.1007/s00170-017-0897-6.
44) H.M. Zakaria, "Microstructural and corrosion behavior of al / sic metal matrix composites," *Ain Shams Eng J*, **5** (*3*) 831–838 (2014). doi:10.1016/j.asej.2014.03.003.
45) L. Sousa, A.C. Alves, A. Guedes, and F. Toptan, "Corrosion and tribocorrosion behaviour of ti-b4c composites processed by conventional sintering and hot-pressing technique," *J Alloys Compd*, **885** 161109 (2021). doi:10.1016/j.jallcom.2021.161109.
46) V. V Popov, A. Pismenny, N. Larianovsky, A. Lapteva, and D. Safranchik, "Corrosion resistance of al – cnt metal matrix composites," 1–12 (2021).
47) P. Mansoor, and S.M. Dasharath, "Materials today : proceedings a review paper on magnesium alloy fabricated by severe plastic deformation technology and its effects over microstructural and mechanical properties," *Mater Today Proc*, **45** 356–364 (2021). doi:10.1016/j.matpr.2020.10.1014.
48) K. V. Mahendra, and K. Radhakrishna, "Characterization of stir cast al-cu-(fly ash + sic) hybrid metal matrix composites," *J Compos Mater*, **44** (*8*) 989–1005 (2010). doi:10.1177/0021998309346386.
49) S. Kumar, N. Alok, and S. Sisir, "Impact of process parameters on solid particle erosion behavior of waste marble dust - filled polyester composites," *Arab J Sci Eng*, **46** (*8*) 7197–7209 (2021). doi:10.1007/s13369-020-05175-1.
50) J.F. Flores, A. Neville, N. Kapur, and A. Gnanavelu, "Corrosion and erosion-corrosion processes of metal-matrix composites in slurry conditions," *J Mater Eng Perform*, **21** (*3*) 395–405 (2012). doi:10.1007/s11665-011-9926-z.
51) M.S. Ozerov, M. V Klimova, N.D. Stepanov, and S. V Zherebtsov, "MICROSTRUCTURE evolution of a

ti / tib metal-matrix composite during high-temperature deformation," **38** 54–63 (2018).
52) L. Urtekin, G. Kucukturk, T. Karacay, I. Uslan, and S. Salman, "An investigation of thermal properties of zirconia coating on aluminum," 2323–2332 (2012). doi:10.1007/s13369-012-0289-z.
53) S. Ozturk, "Machinability of stellite-6 coatings with ceramic inserts," 7375–7383 (2014). doi:10.1007/s13369-014-1343-9.